International Journal of Mining, Reclamation and Environment
Publication details, including instructions for authors and subscription information:
http://www.informaworld.com/smpp/title~content=t713658227

Human health risk assessment in regions surrounding historical mining activities: the effect of change of support

A. Korre [a]; J. R. Gay [b]; S. Durucan [a]
[a] Department of Earth Science and Engineering, Royal School of Mines, Imperial College London, London, UK [b] Health Protection Agency, Centre for Radiation, Chemical and Environmental Hazards, Chilton, Didcot, UK

First Published on: 28 June 2007

To cite this Article Korre, A., Gay, J. R. and Durucan, S.(2007)'Human health risk assessment in regions surrounding historical mining activities: the effect of change of support',International Journal of Mining, Reclamation and Environment,21:3,219 — 239
To link to this Article: DOI: 10.1080/17480930701390297
URL: http://dx.doi.org/10.1080/17480930701390297

International Journal of Mining, Reclamation and Environment
Vol. 21, No. 3, September 2007, 219–239

Taylor & Francis
Taylor & Francis Group

Human health risk assessment in regions surrounding historical mining activities: the effect of change of support

A. KORRE*†, J. R. GAY‡ and S. DURUCAN†

†Department of Earth Science and Engineering, Royal School of Mines, Imperial College London, London, UK
‡Health Protection Agency, Centre for Radiation, Chemical and Environmental Hazards, Chilton, Didcot, UK

This paper presents a probabilistic exposure model and its adaptation for use with spatially explicit information: soil contaminant concentrations and pH levels, predicted by geostatistical simulation; and population data mapped according to place of residence. Sequential indicator simulation (SIS) is used to provide 1000 plausible maps of soil contaminant concentrations, and results are fed into the exposure model to produce risk maps. Distributions of exposure values are closely related to uncertainty in the soil contaminant values. Using a different support for the estimations has a large effect on the results when comparing exposure values to regulatory cut-offs. Mapping the number of overexposed people allows effective targeting of clean up to reduce efficiently the number of overexposed individuals. Two areas of historical mining activity, a case study from the Southern Urals region of Russia for metal mining and another study from the Tula coal mining region of Russia, are used to demonstrate the importance of the support in the human health risk evaluation.

Keywords: Geostatistics; Risk assessment; Contaminated land; Mining

1. Introduction

In the past, risk assessments have been to some extent qualitative, rating sites simply as high, medium or low risk. More recently, the methodologies developed focus on more quantitative risk assessments which not only give a numerical estimation of the risk, but also attach some measure of the uncertainty in the numeric estimation, for instance, by attaching a confidence interval to the estimate. In such cases, the results may be presented as the risk of one additional cancer death per million population, or the probability of a person exceeding the tolerable daily soil intake (a dose which is deemed to present no health risk).

*Corresponding author. Email: a.korre@imperial.ac.uk

International Journal of Mining, Reclamation and Environment
ISSN 1748-0930 print/ISSN 1748-0949 online © 2007 Taylor & Francis
http://www.tandf.co.uk/journals
DOI: 10.1080/17480930701390297

A further improvement has been a move away from deterministic assessments to probabilistic ones. A deterministic risk assessment uses a point value for each variable in the risk equation, e.g. the average soil concentration and the average bodyweight of the receptor, whereas a probabilistic assessment takes into account the variability of natural phenomena and uncertainty in measurements. Some variables in the risk equation have a distribution of plausible values and using probabilistic methods, like Monte Carlo methods, by repeatedly sampling the input distributions and feeding the values into the risk model, a distribution of plausible answers is produced. This distribution captures the uncertainty and contains much added information for the risk manager, who can see the average, maximum and minimum likely exposure results for the population in question.

One deficiency in many of these models is that the spatial dimension is neglected when calculating the risks. Land contamination often occurs in hotspots, and it is therefore inadequate to assume that the whole population is exposed to the same, maybe average, soil contaminant level. Of the quantitative and spatially-evaluated methodologies in the literature, most are geared towards ecological assessment (Clifford *et al.* 1995, Hope 2001, Kooistra *et al.* 2001, Linkov *et al.* 2001), while the few that deal with human risk calculate and map hypothetical risks in each cell of a gridded map, assuming that a 'critical receptor' resides there (Tristan *et al.* 2000, Korre *et al.* 2002).

This work, on the other hand, uses a probabilistic exposure model developed by the authors (Gay and Korre 2006) which utilizes spatially explicit information: soil contaminant concentrations and pH values predicted by geostatistical simulation; and population numbers mapped according to place of residence. The likely exposure of the population to the contaminant in the top soil, measured in milligrams per kilogram of bodyweight per day [mg (kg^{-1} BW) d^{-1}], is calculated.

This spatial method, however, is subject to the well known phenomenon of support effect, whereby calculations on a larger support (size of the area that corresponds to each prediction) are subject to less variance than those on a smaller support. The exposure results may therefore appear better or worse, simply by consequence of the support size.

This paper demonstrates the importance of agreeing a support size in advance of the risk assessment, since judicious choice of support could enable a risk assessor to tailor the results to better suit the cause. For similar reasons, agreeing which percentile of the distribution of results to use in making decisions is also important. Results are presented in the form of probability distributions and risk maps.

A case study from the Southern Urals metal mining region of Russia is used to demonstrate the effect of support size on a calculation of potential human health risks due to exposure to metal (Ni) contaminated soils. A second case study from the Tula coal mining region of Russia is used to illustrate the approach for Cd exposure which is pH dependent.

2. Methodology

The terms 'exposure' and 'intake' are often used in the literature in conflicting ways. In this paper, the authors follow the precise definitions used in a UK report by the Department of Environment, Food and Rural Affairs and Environment Agency (DEFRA & EA 2002) as follows:

Exposure: the amount of chemical in a medium that is available for intake by the population; expressed in mg kg^{-1}.
Intake: the amount of chemical entering or contacting the human body at the point of entry; expressed in mg (kg^{-1} BW) d^{-1}.

The process for quantitatively assessing risks from contaminated land, in a manner which preserves the spatial distribution of the risks and also gives a measure of uncertainty in the estimations, starts with collection and analysis of soil samples from the site in question. Using geostatistical methods, it is possible to predict and map the soil contaminant concentration across the entire site. Following this, there are two levels at which risk to human health from contaminated land may be evaluated. First, one may quantify the contaminant concentration in the soil (mg kg^{-1}) and compare it to a regulatory cut-off level deemed 'safe' or 'acceptable'; Level 1 in figure 1. This technique has been demonstrated many times (Flatman *et al*. 1985, Leonte and Schofield 1996, Meshalkina 1996, McKenna 1998) and will not be discussed here. Second, one may calculate the human intakes of soil contaminants (mg (kg^{-1} BW) d^{-1}) and compare them to regulatory 'safe' or 'acceptable' intake levels; Level 2 in figure 1. In the spatially-evaluated methodology developed by the authors (Gay and Korre 2006), calculations of the risks at Level 2 are achieved by mapping the local population across the contaminated site, introducing the local population and contaminant data into an intake model and evaluating the results of the intake assessment at each location on the site. Maps are produced to illustrate, for example, counts of people with predicted excess intakes, and may be stratified to show the amount by which the population is in excess of the regulatory 'safe' intake in different places. In this way, the risk manager is supplied with maps detailing where the greatest number of people are at risk from soil contamination and by how much they exceed 'safe' intake levels, thus enabling the manager to target resources efficiently.

Figure 2 is a visual summary of the stages undertaken in the newly proposed spatially-evaluated risk assessment methodology (Gay and Korre 2006), to aid the reader during the sections which follow.

2.1 *Exposure calculation*

Exposure was modelled by the UK Contaminated Land Exposure Assessment (CLEA) algorithm which models intake via three routes: inhalation; dermal absorption; and oral intake (DEFRA &

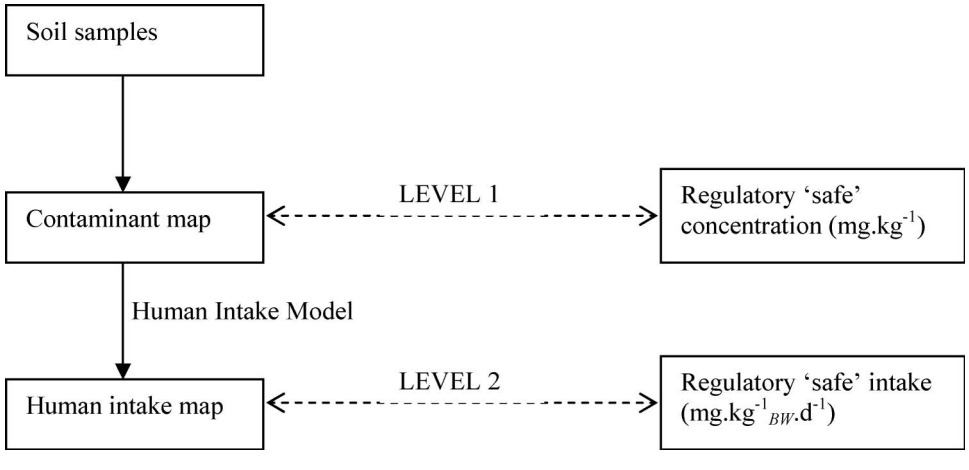

Figure 1. Two levels of approach to the assessment of risks to human health from contaminated land.

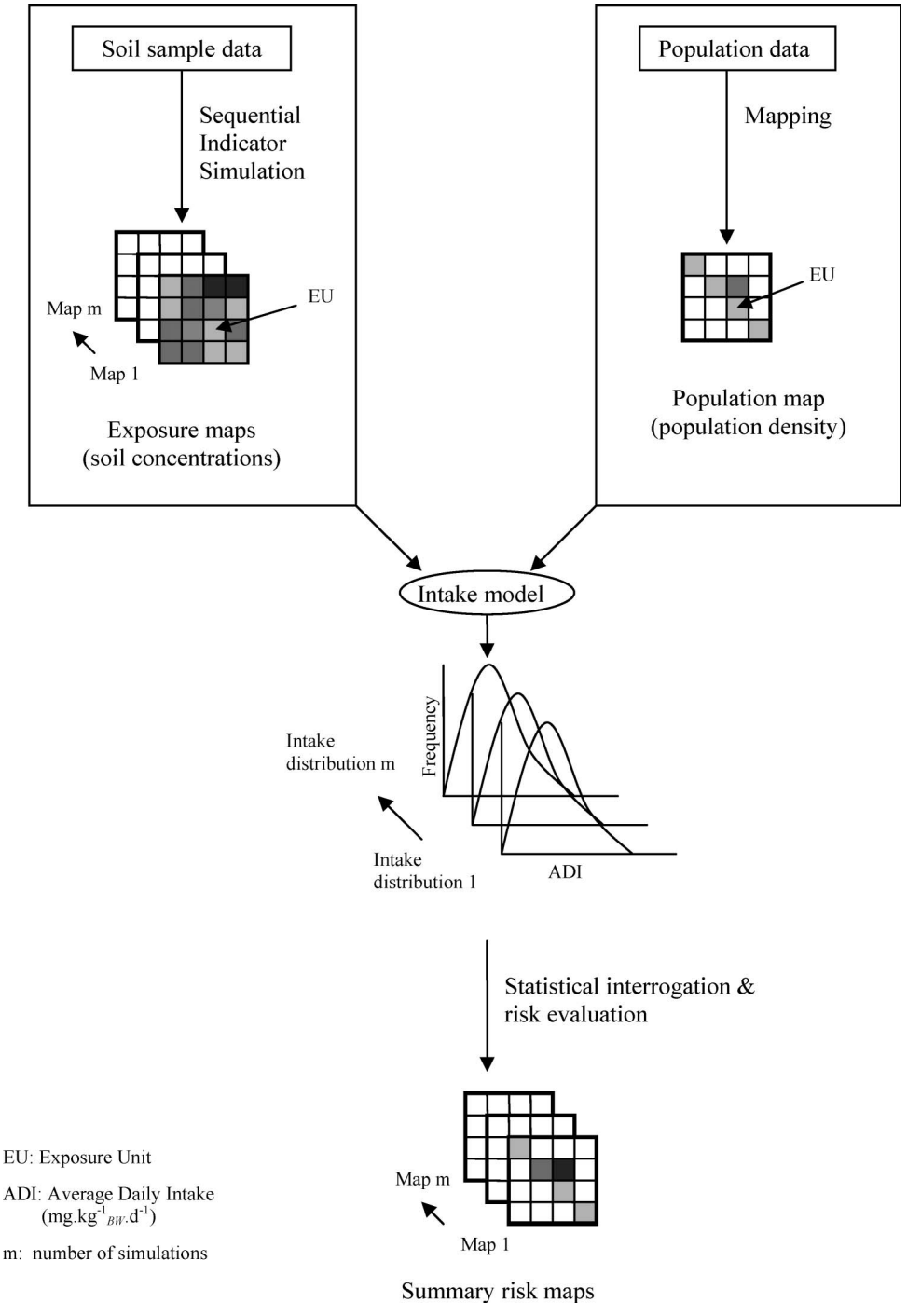

Figure 2. Stages of the spatially-evaluated probabilistic intake assessment methodology.

EA 2002). However, less than 1% of soil Ni (DEFRA & EA 2002) or soil Cd (DEFRA & EA 2002) is taken in via the inhalation and dermal routes, and therefore, only exposure through the oral pathway is calculated as follows:

$$\mathrm{ADE} = \frac{(\mathrm{IR}_{\mathrm{oral}} \times \mathrm{EF}_{\mathrm{oral}} \times \mathrm{ED}_{\mathrm{oral}})}{\mathrm{BW} \times \mathrm{AT}} \tag{1}$$

where

$$\mathrm{IR}_{\mathrm{oral}} = \mathrm{IR}_{\mathrm{dsi}} + \mathrm{IR}_{\mathrm{isi}} + \mathrm{IR}_{\mathrm{veg}} \tag{2}$$

and

$$\mathrm{IR}_{\mathrm{dsi}} = C_{\mathrm{soil}} \times \mathrm{SDR} \tag{3}$$

$$\mathrm{IR}_{\mathrm{isi}} = C_{\mathrm{soil}} \times \sum_{\mathrm{veg}\ \mathit{type}} \left(\mathrm{CR}_{\mathrm{veg}} \times \mathrm{BW} \times \mathrm{HF}_{\mathrm{veg}} \times \mathrm{SL}_{\mathrm{veg}}\right) \tag{4}$$

$$\mathrm{IR}_{\mathrm{veg}} = C_{\mathrm{soil}} \times \sum_{\mathrm{veg}\ \mathit{type}} \left(\mathrm{CR}_{\mathrm{veg}} \times \mathrm{BW} \times \mathrm{HF}_{\mathrm{veg}} \times \mathrm{CF}_{\mathrm{veg}}\right) \tag{5}$$

where

ADE: average daily exposure to a chemical from soil [mg (kg^{-1} BW) day^{-1}]
IR: chemical exposure rate (mg day^{-1})
C_{soil}: contaminant concentration in soil (mg g^{-1})
SDR: average daily soil and dust ingestion rate (g day^{-1})
BW: bodyweight (kg)
CR_{veg}: consumption rate per vegetable (g FW day^{-1})
HF_{veg}: fraction per vegetable that is home grown (−)
SL_{veg}: amount of attached soil per vegetable (g g^{-1} FW)
CF_{veg}: calculated soil to plant concentration factor ($\mu g\ g^{-1}$FWplant/$\mu g\ g^{-1}$DWsoil)

Of the inputs to the model, SDR (pre-school children only), BW, CR_{veg} and HF_{veg} are treated probabilistically. In the CLEA methodology, C_{soil} is treated deterministically, i.e. a single value is taken to be representative of the soil contaminant value. The CLEA methodology was modified so that C_{soil} is treated probabilistically and spatially (Gay and Korre 2006). The original methodology developed by the authors (Gay and Korre 2006) assumes that the intake of contaminant is independent of soil pH, which is not necessarily correct in all cases. For example, cadmium (Cd) intake is pH dependent: the lower the pH, the higher the soil to plant concentration factor (CF_{veg}) and hence the higher the likely human intake. For this reason, for Cd intake CF_{veg}, is also treated probabilistically by linking it to pH via the following regression equations (DEFRA & EA 2002):

$$\text{Root veg}: \ \ln(\mathrm{CF}) = 11.174 - (1.6461 \times \mathrm{pH}) \tag{6}$$

$$\text{Leafy veg}: \ \ln(\mathrm{CF}) = 11.206 - (1.634 \times \mathrm{pH}) \tag{7}$$

Exposures can be calculated by assuming that home grown vegetables are consumed, or not. Assuming no home grown vegetable consumption for the Cd intake has the advantage of removing the pH dependent factor, difference in exposure at the two supports will be solely due to changes in soil Cd and the support effect can be clearly demonstrated. Including home grown vegetable consumption, on the other hand, will likely give a more realistic assessment of exposure for a study area, particularly, when it is known that a large proportion of the population assessed consume their own vegetable produce. This is specifically significant since vegetable intake, rather than direct soil/dust ingestion, is the major source of Cd intake (Moir and Thornton 1989, DEFRA & EA 2002).

The population was kept identical for all three scenarios examined (50 m EU, 500 m EU and nonspatial) in each of the case studies, in as much as all the probabilistic population variables selected for simulation one would be the same in all three scenarios, and those for simulation two would be the same in all three scenarios and so on for each of the 1000 simulations. The only differences in calculations were the C_{soil} values for the Ni case study and C_{soil} and CF_{veg} values for the Cd case study, which depended upon the support size used.

2.2 *Risk estimation*

First, geostatistical sequential indicator simulation (SIS) is used to provide 1000 plausible maps of soil concentrations for Ni or Cd on a grid. In the case of Cd exposure, this process was repeated for soil pH values. One cell is assumed to be the 'exposure unit' (EU) such that a person inhabiting that cell is assumed to be exposed to that concentration of soil metal on a daily basis over the period of a year. Next, the population in each settlement is allocated to one of these exposure units. Finally, 1000 chronic intake values are calculated for each person in the population by means of a probabilistic exposure equation which uses the 1000 EU soil concentrations (for Ni and Cd) and pH levels (for Cd) as inputs in the EU to produce a distribution of 1000 possible exposures for each person.

Next the EU size is changed to a 10 times larger square. The average soil concentration for that square is calculated by averaging the values for the 100 original size cells and the population of the original 100 EUs is now exposed to the larger EU average soil value. Lastly, the whole region is taken as the EU, and the whole population is assumed to be exposed to the average soil concentration for the region. This, in effect, is a nonspatial assessment.

On the basis of the original soil sampling density, the assessment is made on a 50×50 m^2, a 500×500 m^2 as well as the whole region for Ni in the Southern Urals. For Cd in the Tula region, the EU support effect is investigated by working on a 25×25 m^2 grid then a 250×250 m^2 grid and by using the whole site average.

The seriousness of the estimated exposures is assessed by comparing the results to an advisory Tolerable Daily Soil Intake.

3. Case studies

3.1 *Nickel exposure and risk assessment: Gai region*

The Gai copper-zinc-pyrite deposit is situated in the Orenburg region of the Southern Urals in Russia and has been mined since 1959. 85–90% of mining takes place underground (figure 3). Dressing and metallurgical processing is also carried out in the region and spoil heaps are evident in the vicinity of the villages and towns. There are four settlements in the study area, three villages (Kalinovka, Kameinino and Popovka) and a town (Gai), with a total population of about 35 000.

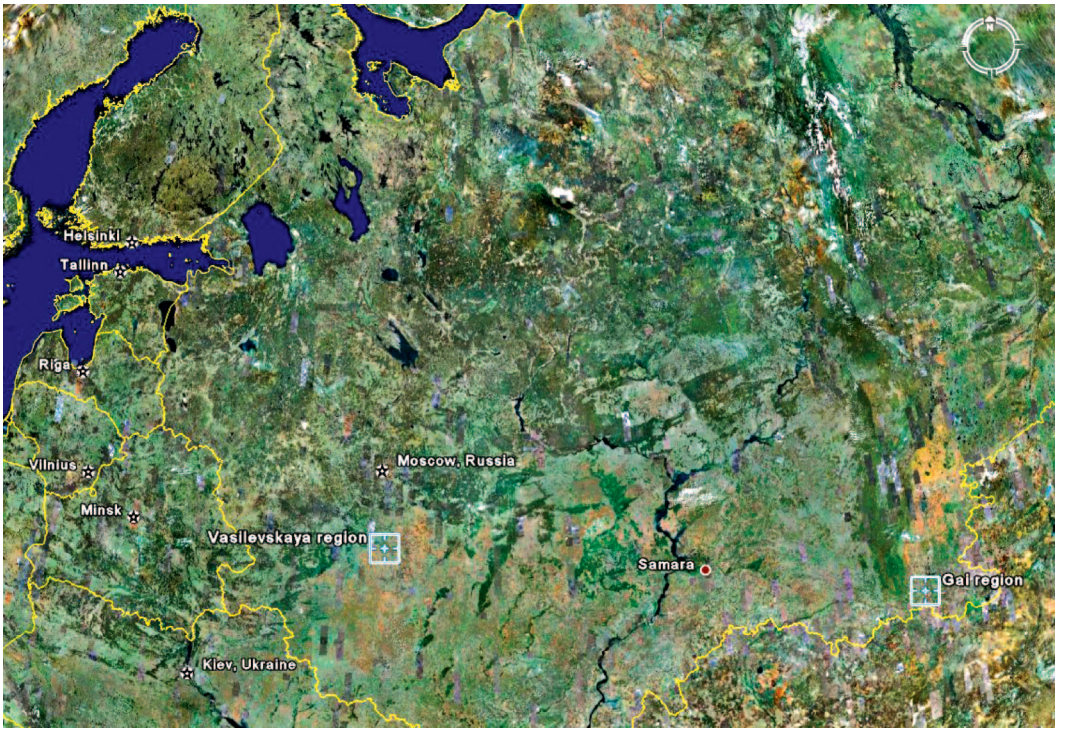

Figure 3. Map showing the location of the two case studies, Gai and Vasilevskaya regions in Russia.

Table 1. Statistics of Ni sample distribution.

Statistic	Ni (mg kg^{-1})
Mean	74
SD	79
Min	18
5%	31
Median	64
95%	108
99%	280
Max	981
TAC	80

TAC shown for reference.

By way of illustrating the methodology, Ni exposure was investigated. Ni can be a cause of dermatitis and, more seriously, reproductive problems including spontaneous abortion and malformations. Russian 'Tentative Allowable Concentrations' (TAC) are advisory concentrations meant to be protective of agricultural soils (Hygienic Standards 1995). Of 160 topsoil samples taken in the region, 24% exceeded the TAC of 80 mg kg^{-1}. Table 1 shows the statistics for the Ni soil samples, and figure 4 shows a map of the Gai region. No regulatory concentrations that are

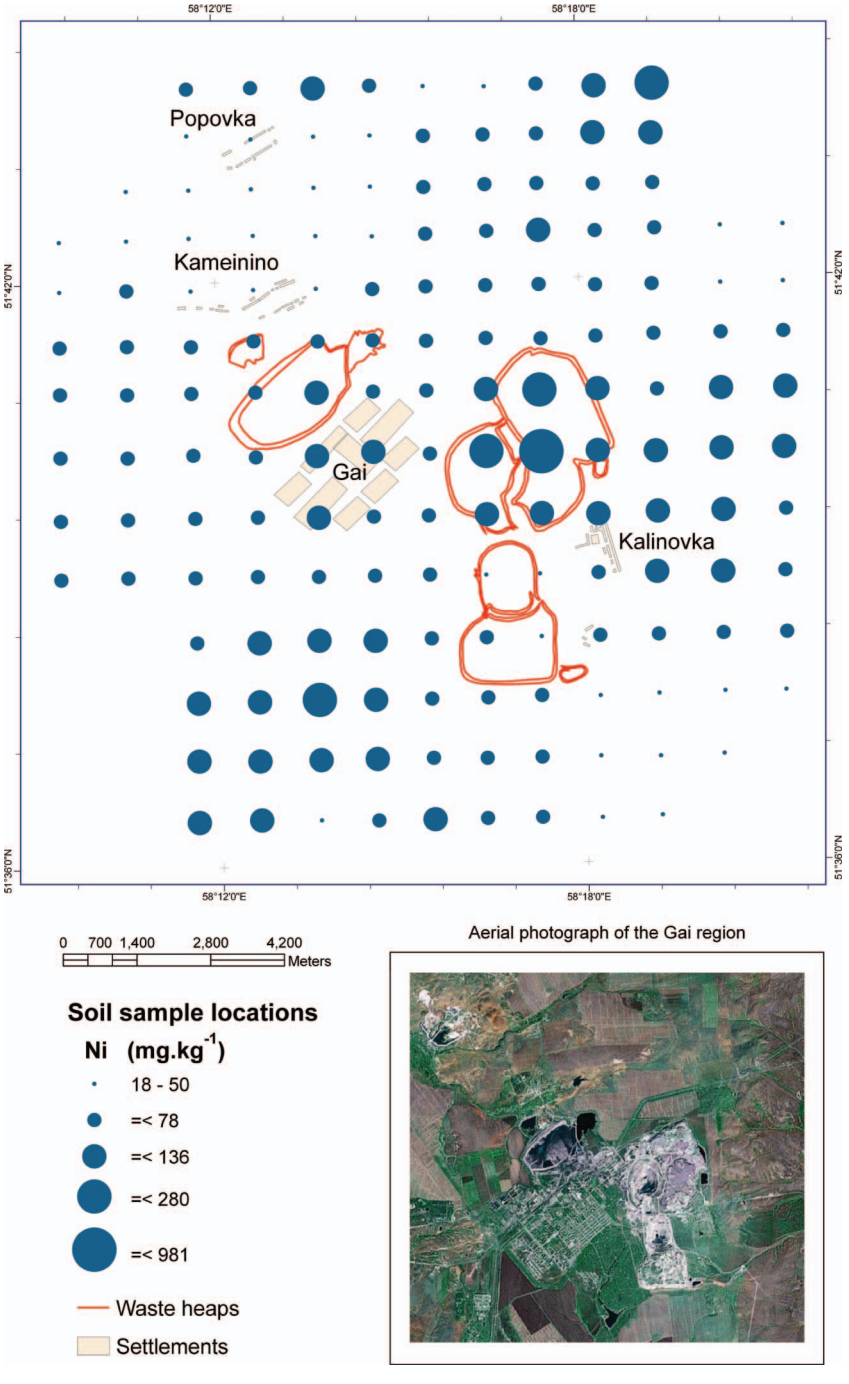

Figure 4. Gai mining region showing settlements, position of the waste tips, the locations and measured concentrations (mg kg^{-1}) for Ni samples.

specifically health-protective were found in Russian regulations; therefore, the UK regulatory 'Tolerable Daily Intake' (TDI) was used as a basis for the health risk assessments.

SIS was undertaken to provide 1000 plausible soil maps. The set of maps represents the uncertainty in the soil concentrations, and the uncertainty in each EU is represented by the distribution of 1000 values for that cell. Omnidirectional indicator variograms were fitted at the nine decile values of the sample data: 39, 46.5, 56.5, 61.5, 63.5, 67, 74, 85 and 99 mg kg^{-1}. The variogram models, fitted using Isatis (Geovariances 2007), were composed of nugget, exponential and/or spherical components. Simulations were carried out with GSLIB's SISIM routine (Deutsch and Journel 1998) on a 50×50 m^2 square grid with 290 cells in each direction. Minimum and maximum allowable Ni concentrations were set to 10% less and 10% more than the minimum and maximum sample values, respectively (i.e. to 16 mg kg^{-1} and 1080 mg kg^{-1}), assuming that it was unlikely that the minimum and maximum values would have been found in sampling. The figure of 10% is arbitrary, but may well lead to more realistic simulations.

The results obtained on the 50×50 m^2 grid were converted into the 500×500 m^2 grid by averaging the 100 smaller values inside each larger cell. They were also averaged to produce a global average for the whole site. This was to assess if the support effect from the geostatistical calculations had an impact on the results of the exposure calculation.

Population numbers, split by age group (0–5 years, 6–17 years and 18+ years), are known for each settlement and are given in table 2. Exact coordinate locations of the population were unavailable; therefore, individuals were allocated to 50×50 m^2 EUs in as logical a manner as possible. This was done by marking the grid cells in each settlement which contained buildings, then dividing the population for each settlement between the occupied cells in as near uniform manner as possible (ensuring no fractions of people existed). The numbers were aggregated up for the 500×500 m^2 EUs.

The Tolerable Daily Soil Intake (TDSI) is a regulatory value used in the UK, and ADEs calculated for the population in the Gai region are compared to this value as an indication of the seriousness of the exposures experienced. A Tolerable Daily Intake (TDI) of 5 μg (kg^{-1} BW) d^{-1} is specified for Ni intake (DEFRA & EA 2002). The mean daily intake from background sources, which is age dependent, is subtracted from the TDI to give the TDSI, e.g. 2.7 μg (kg^{-1} BW) d^{-1} for an adult weighing 70 kg. ADE for each individual is compared to its estimated TDSI and the number of the population exceeding the TDSI is calculated.

3.1.1 Ni risk assessment results and discussion. There are 1000 ADE outcomes for each person. Box and whisker plots in figures 5 to 7 represent the distribution of upper 95th percentile (P95) values for each person, split by age category: figure 5 shows results for 0–5-year olds; figure 6 for ages 6–17 years; and figure 7 for ages 18+. The lines represent (from top to bottom) maximum, P75, P50, P25 and minimum, triangles represent the mean ADE [mg (kg^{-1} BW) d^{-1}]. Figures 8(a) to 8(c) show the distribution of estimates, from the 1000 simulations, for the fraction of the total population that exceeds the TDSI.

Table 2. Population distribution in the four settlements in the Gai region.

	Gai	Kalinovka	Kameinino	Popovka
Infant	2540	8	22	12
School age	5760	12	35	26
Adult	26 076	55	263	188

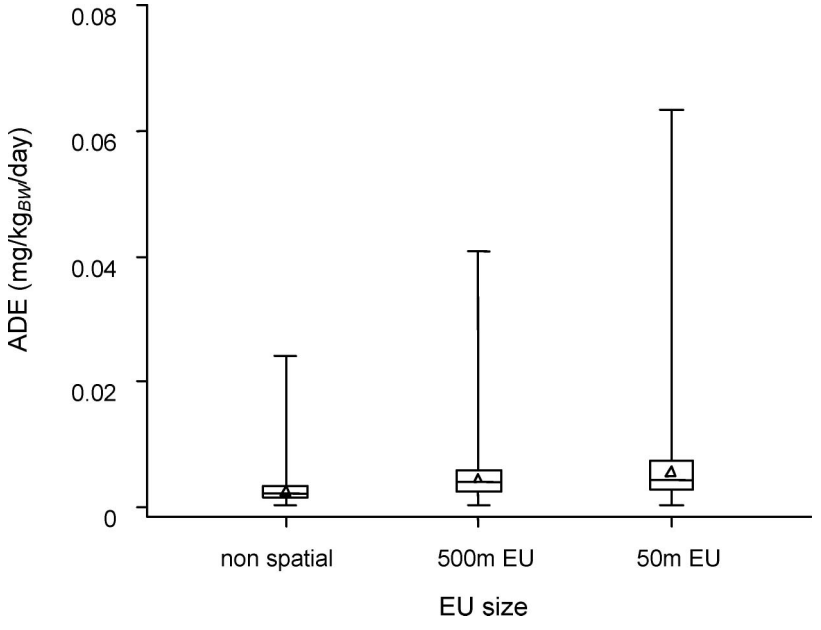

Figure 5. Distributions of P95 of Ni ADE estimates for infants using different support sizes in the Gai region ($n = 2582$).

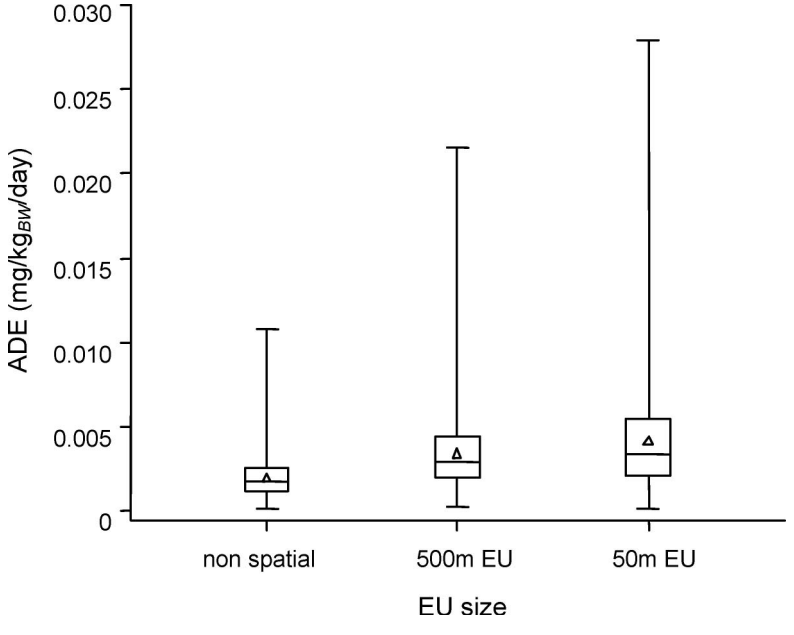

Figure 6. Distributions of P95 of Ni ADE estimates for school-age children using different support sizes in the Gai region ($n = 5833$).

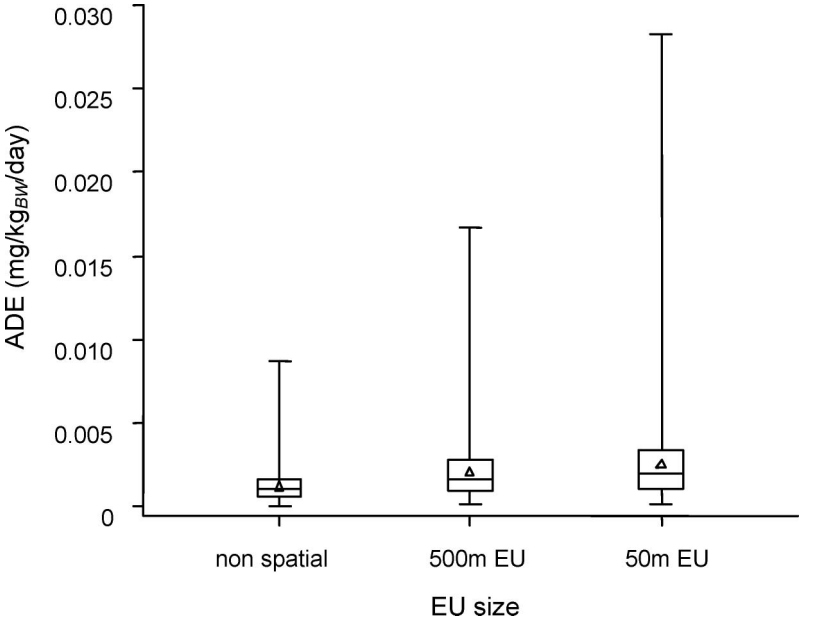

Figure 7. Distributions of P95 of Ni ADE estimates for adults using different support sizes in the Gai region ($n = 26\ 582$).

The maps in figure 9 show the spatial distribution of the number of people exceeding the TDSI calculated at two different supports (500 m and 50 m EUs). The P95 estimate is shown for each cell. The 50 m results have been aggregated into 500 m cells purely for display purposes and for ease of comparison.

Figures 5 to 7 clearly show a difference between the results calculated with a different support size, taken here to be representative of the EU (exposure unit). The figures show the upper 95th percentile estimates for ADE (average daily exposure) for each person in the population after 1000 simulations. Using the average simulated soil value for the entire area leads to less uncertain results, and the uncertainty increases through the 500 m to the 50 m EU size. The interquartile ranges in figures 5 to 7 increase with decreasing support size, as do the upper extremes.

Figure 6 (school-age children) and figure 7 (adults) are of a more similar magnitude than figure 5 (infants). This is due to large differences in behaviour for babies and small children. They experience many more hand to mouth contacts than older age groups and are more likely to mouth any object put before them increasing their direct (inadvertent) soil and dust intake (SDR).

Similar plots of median ADE (not shown) are less markedly different than those of the P95 values. Again, the school-age children and adults are of a similar magnitude, and infants about twice as high. In this case, however, the median 500 m EU values are very slightly higher than the 50 m EU values. This may be due to the support effect increasing the lower soil values, thus pushing up the median estimates.

Other factors playing a part are the spatial position of the population and the person-specific variables such as bodyweight (BW). It may be the case that a person residing in a 50 m EU is exposed to a very small Ni concentration and another in the adjacent EU is exposed to a very high concentration. Despite this, they may receive the same dose of Ni, because of other factors like BW: for equivalent concentrations of Ni, a small bodyweight leads to a higher dose [mg $(kg^{-1}$ BW $d)^{-1}$] than a large bodyweight. Therefore, a small person exposed to a low

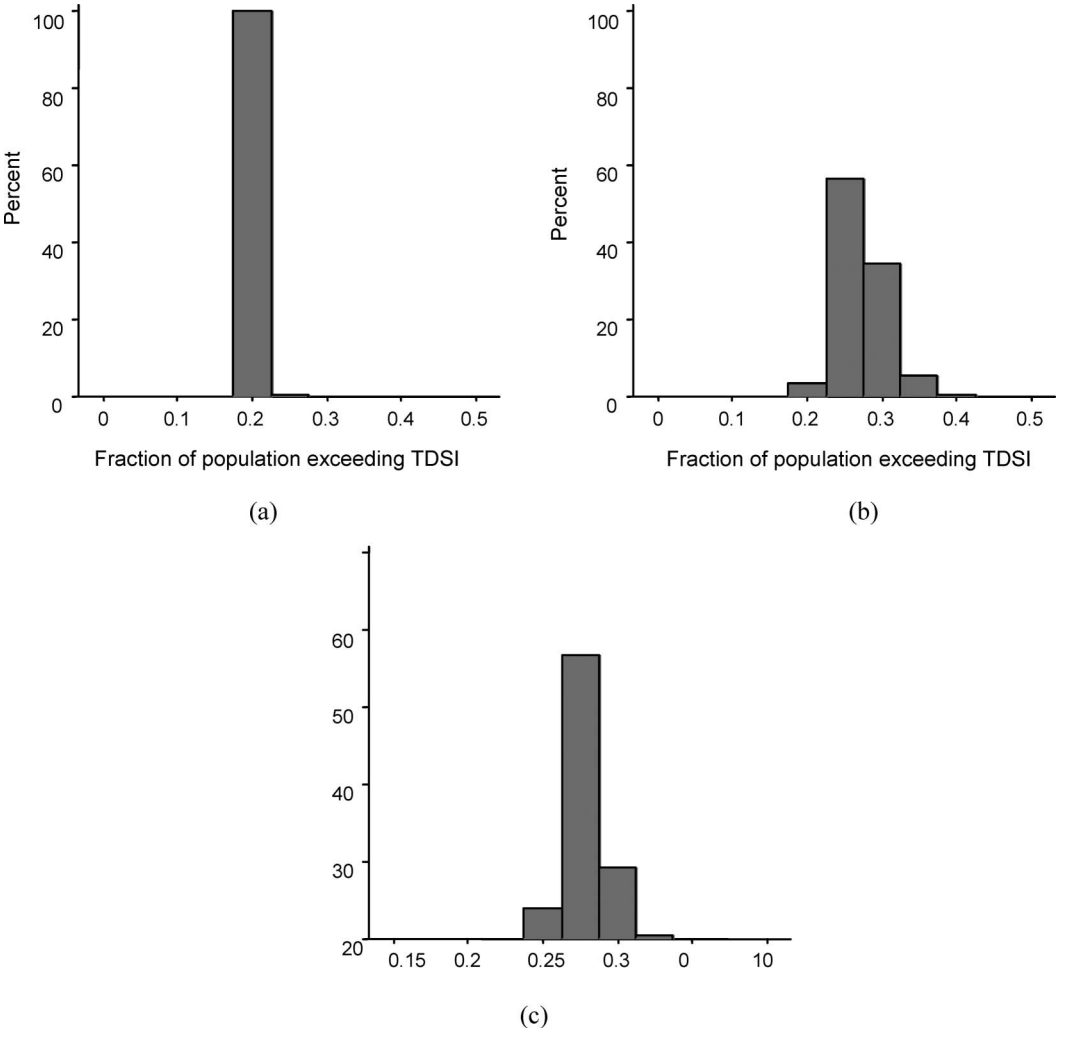

Figure 8. Proportion of the population which exceeds the Ni TDSI in the Gai mining region: (a) calculated nonspatially, (b) calculated for 500 m EUs and (c) calculated for 50 m EUs. (Distribution of results from 1000 simulations.)

concentration could experience the same dose as a large person exposed to a high concentration. It is possible when changing support to 'move' persons from either low or high Ni concentrations to a more average concentration, but the effect of this change on exposure will be affected also by other parameters particular to that individual.

The stark difference in the P95 estimates is important. Regulators often use the P95 value as a 'reasonable maximum' value when assessing risks (USEPA 1989). Figures 8(a) to 8(c) show the distribution (after 1000 simulations) of the estimated percentage of the population which exceeds the TDSI. Nonspatial assessment, using an average soil value, leads to a very tight, maybe over-confident, estimate that around 20% of the population is overexposed. Assuming a 500 m square EU suggests that around 20–40% of the population is overexposed, while assuming a 50 m square EU suggests a figure of around 20–35%. In this case, the 500 m support leads to a more

uncertain estimate of exposure than the 50 m support, despite the simulated soil values being more uncertain at the 50 m support level. This may be due to the spatial position of the population. It is possible that no population resides in the cells with the most extreme soil values, or the individuals that do reside in these cells, do not suffer extreme exposure because of other variables that affect their exposure levels being more 'average'. Another reason that there appears to be more people exceeding the TDSI at the 500 m EU size than at the 50 m EU size could be the position of the TDSI within the distribution of the ADE estimates for each individual. Even though the calculated ADEs may be more variable at the smaller EU size, at the larger EU size the support effect may have the result in raising all the lower estimated soil values, increasing the ADE estimates and therefore pushing more of the 'low' estimates over the TDSI limit. In this case, we are not concerned with how much in excess the exposure is, rather just that it is, so we may have lots of 'small' overexposures at the 500 m EU size rather than fewer 'large' overexposures at the 50 m EU level.

Figure 9 maps out the places where excess exposures occur. The numbers plotted are the P95 estimates. Again, using these extremely high values highlights differences due to support, whereby there are more people in excess of the TDSI when calculated at the smaller support than at the larger support.

Some regulators produce regulatory guidelines theoretically based on the protection of the 95th percentile of the population (a 'reasonable maximum) (DEFRA & EA 2002), and so it may be of

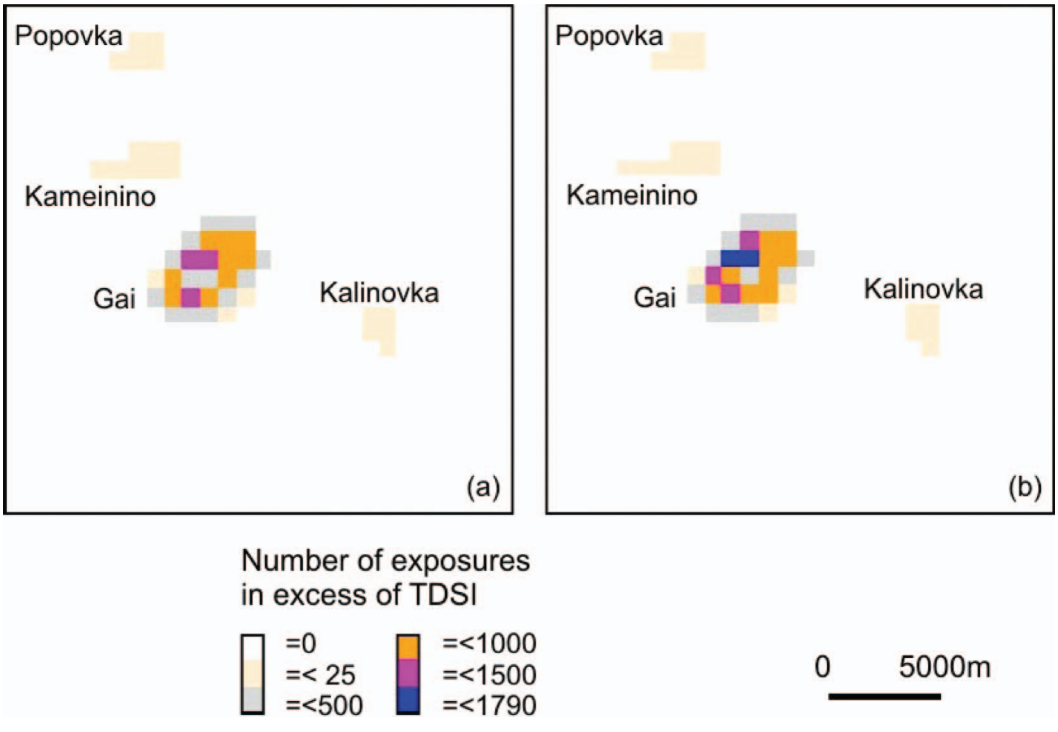

Figure 9. P95 estimate of the number of the population in each 500 m cell that are exposed in excess of the Ni TDSI in the Gai region; (a) calculated on a 500-m grid; (b) calculated on a 50-m grid and aggregated for a clearer comparison.

interest to clean a site to a level that, in theory, protects 95% of the population. It is necessary to know where the population is positioned in order to target clean up in the right places.

The highest number of excesses occurs in the city. This could be due to high soil concentrations or the fact that there is a high population density there, or a combination of the two. In a village, for example, even if the soil concentration is high, there are few people that the excesses may not seem unreasonable. If one wishes to protect 95% of the whole population in the region as a reasonable target, it may be more efficient to clean slightly contaminated soils in the city, where more people are exposed, than extremely contaminated soils in the villages where few people are exposed in order to reduce the exposures of a higher number of people below the TDSI more quickly. This approach seems a somewhat clinical method to meet targets, rather than assessing the size of the excess exposures.

3.2 *Cadmium exposure and risk assessment: Vasilevskaya region*

The Vasilevskaya coal mines lie in the Tula region of Russia, approximately 200 km south of Moscow (figure 3). Both underground and opencast mining methods are used to extract lignite which is processed on site and, consequently, large waste dumps are found in the area. In the study area there are four settlements, relatively small in size, with a total population of 6554 people (figure 10). Cd is toxic to humans, causing renal damage and some types of cancer. Exposure to Cd was investigated since the soil concentration levels in the region are at or around the safe threshold levels: 1 mg kg^{-1} at pH less than 5.5 and 2 mg kg^{-1} at pH over 5.5 (Hygienic Standards 1995).

One hundred and thirty-five topsoil samples were taken across the region and the distributions of the levels of Cd and pH are given in table 3. pH was also measured, since the CF_{veg} variable in the exposure model is pH dependent. The sample positions are shown in figure 10 and the symbols represent the level of Cd in the topsoil.

Three 'non detect' Cd samples were recorded and were changed to be equal to the detection limit of the analytical test (0.1 mg kg^{-1}), so that the range of Cd values becomes 0.1 – 1.9 mg kg^{-1}. Indicators were modelled at the 10th, 19th, 39th, 61st, 78th, and 89th deciles being 0.35, 0.45, 0.55, 0.65, 0.75, and 0.95 mg kg^{-1}, respectively. Isotropic variogram models were fitted using Isatis (Geovariances 2007) and were composed of nugget and spherical components. SIS was undertaken, with the GSLIB SISIM routine (Deutsch and Journel 1998) on a 25×25 m^2 square grid with 330 cells in the east-west direction and 160 north-south. Simulated Cd values were allowed to fluctuate between the detection limit value and 10% higher than the maximum measured sample value: 0.1 and 2.1 mg kg^{-1}, respectively. The results obtained on the 25×25 m^2 grid were converted into the 250×250 m^2 grid by averaging the 100 smaller values inside each larger cell. They were also averaged to produce a global average for the whole site. This was to assess if the support effect from the geostatistical calculations had an influence on the results of the exposure estimation.

The process was repeated for pH. Isotropic variograms were modelled at the 10th, 20th, 31st, 43rd, 53rd, 61st, 72nd, 83rd and 90th percentiles being pH 5.65, 6.05, 6.65, 6.95, 7.15, 7.35, 7.45, 7.55 and 7.65, respectively. Nugget and spherical components were used at the lower deciles and nugget and exponential at the higher deciles. Simulations were allowed to fluctuate between pH 7.9 and pH 4.1.

Population numbers, split by age group (0 – 5 years, 6 – 17 years and 18+ years), are known for each settlement. Exact coordinate locations of the population were unavailable, and therefore, people were allocated to 25×25 m^2 EUs by marking the grid cells in each settlement which contained buildings, then dividing the population for each settlement between the occupied cells in

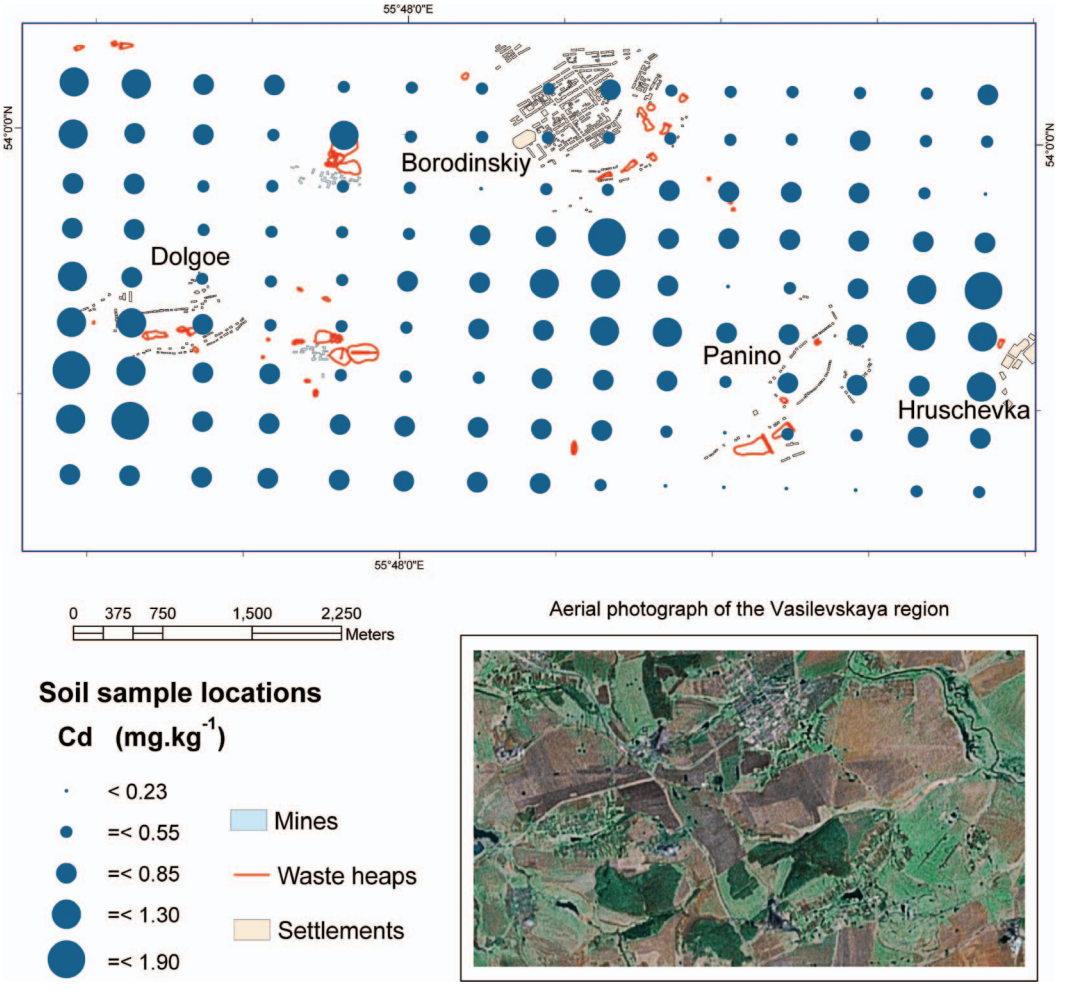

Figure 10. Vasilevskaya mining region showing the settlements, position of the mines and waste tips, the locations and measured concentrations (mg kg^{-1}) for Cd samples.

Table 3. Sample distribution for Cd and pH ($n = 135$).

Statistic	Cd (mg kg^{-1})	pH
Mean	0.6	6.9
SD	0.3	0.8
Min	0.0	4.2
5%	0.2	5.2
Median	0.6	7.1
95%	1.2	7.7
99%	1.9	7.8
Max	1.9	7.8

as near uniform manner as possible (ensuring no fractions of people existed). The numbers were aggregated for the 250×250 m^2 EUs.

3.2.1 Cd risk assessment results and discussion. There are 1000 ADE outcomes for each individual in the population and figure 11 shows the distributions of the 95th percentile (P95) exposure values calculated for each person by age category on the 25×25 m^2 and 250×250 m^2 support. Figure 12 shows the 5th percentile (P5), median (P50) and P95 estimates for the adult age category at each support. Figure 13 shows the distribution of 1000 estimates for percentage of the whole population which exceeds a regulatory 'safe' cut-off, while figure 14 maps the median estimate of overexposed individuals per 250 m EU.

Figure 11 demonstrates the differences in exposure between the age classes, with the 0 – 5-year olds having the biggest P95 ADE estimates. This is due to behavioural patterns seen in youngsters, such as mouthing objects and playing on the floor, which can lead to higher exposures. Though not clear in the youngest age class, it can be seen in the two older age groups that the spread of the ADE estimates is less at the 250 m EU size than the 25 m EU size and this will be a direct result of the smoothing of the soil concentrations by averaging the 25 m EU results for the 250 m results.

Figure 12 shows the support effect in another way, for the adult age class. P5 estimates for the nonspatial, 250 m EU size and 25 m EU size are graphed on cumulative plots. This is repeated for P50 and P95 estimates. Plot (a) shows that the P5 estimates are highest for the nonspatial calculation, followed by the 250 m EU then the 25 m EU. Plot (b) shows the P50 again highest for the nonspatial results, but this time, there is little difference between the 250 m and 25 m EU results until the top end of the distribution, where the 250 m results are slightly higher. P95 values

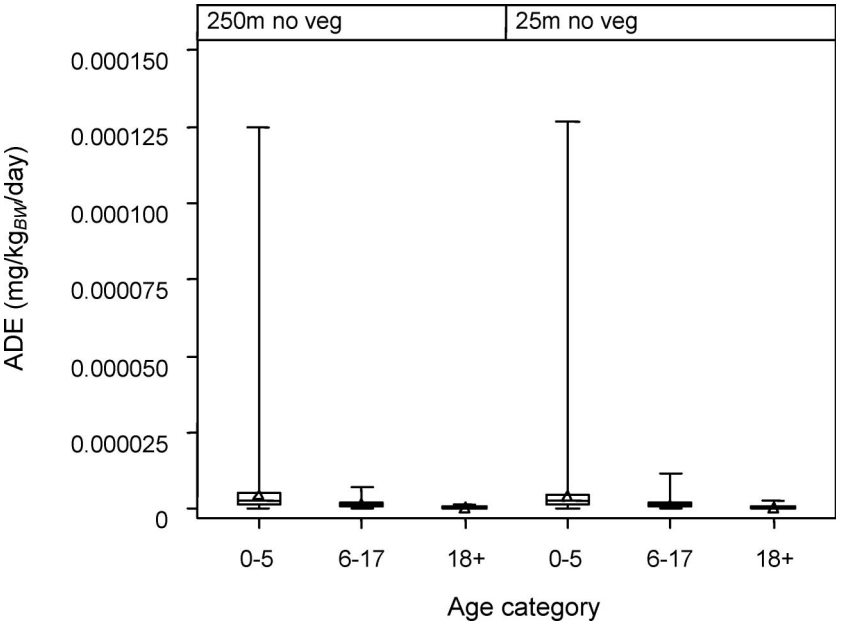

Figure 11. Distribution of P95 ADE estimates in Vasilevskaya region without vegetable consumption after 1000 simulations. Lines represent (from top to bottom) maximum, 75th percentile, median, 25th percentile, and minimum. Triangles represent the mean.

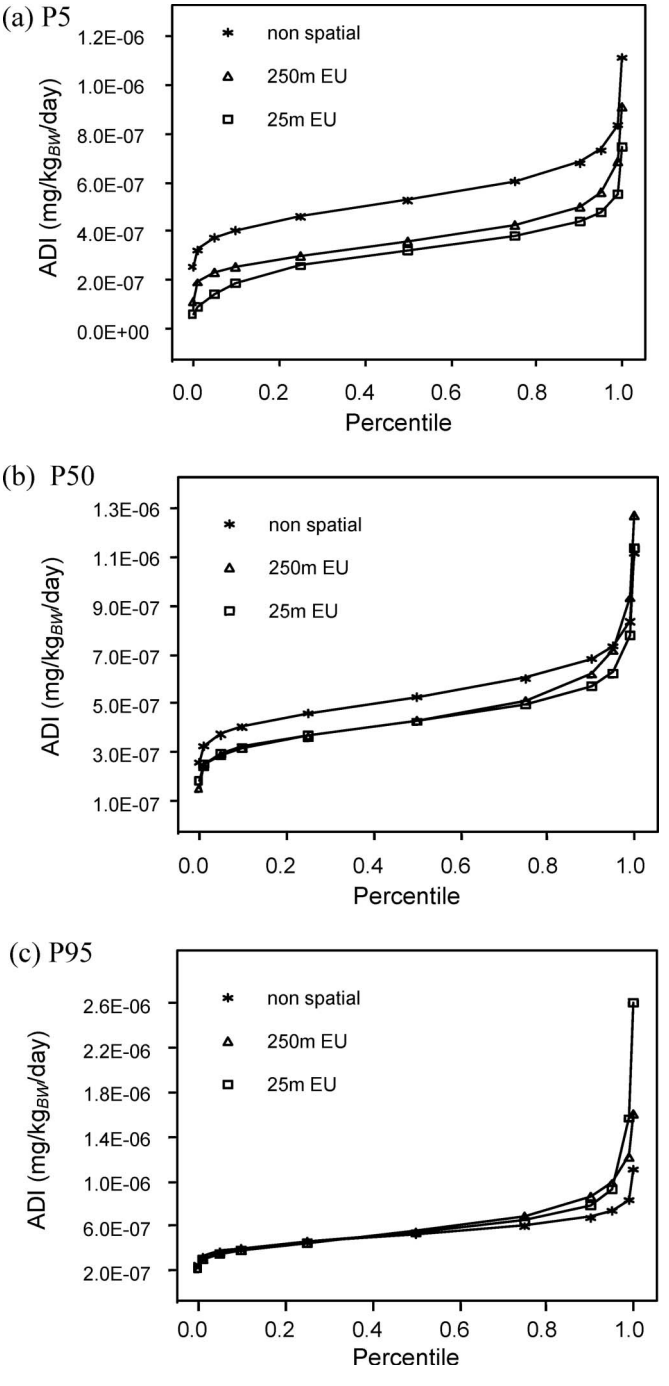

Figure 12. ADE estimates for adults without home grown vegetable consumption on different support sizes in Vasilevskaya region.

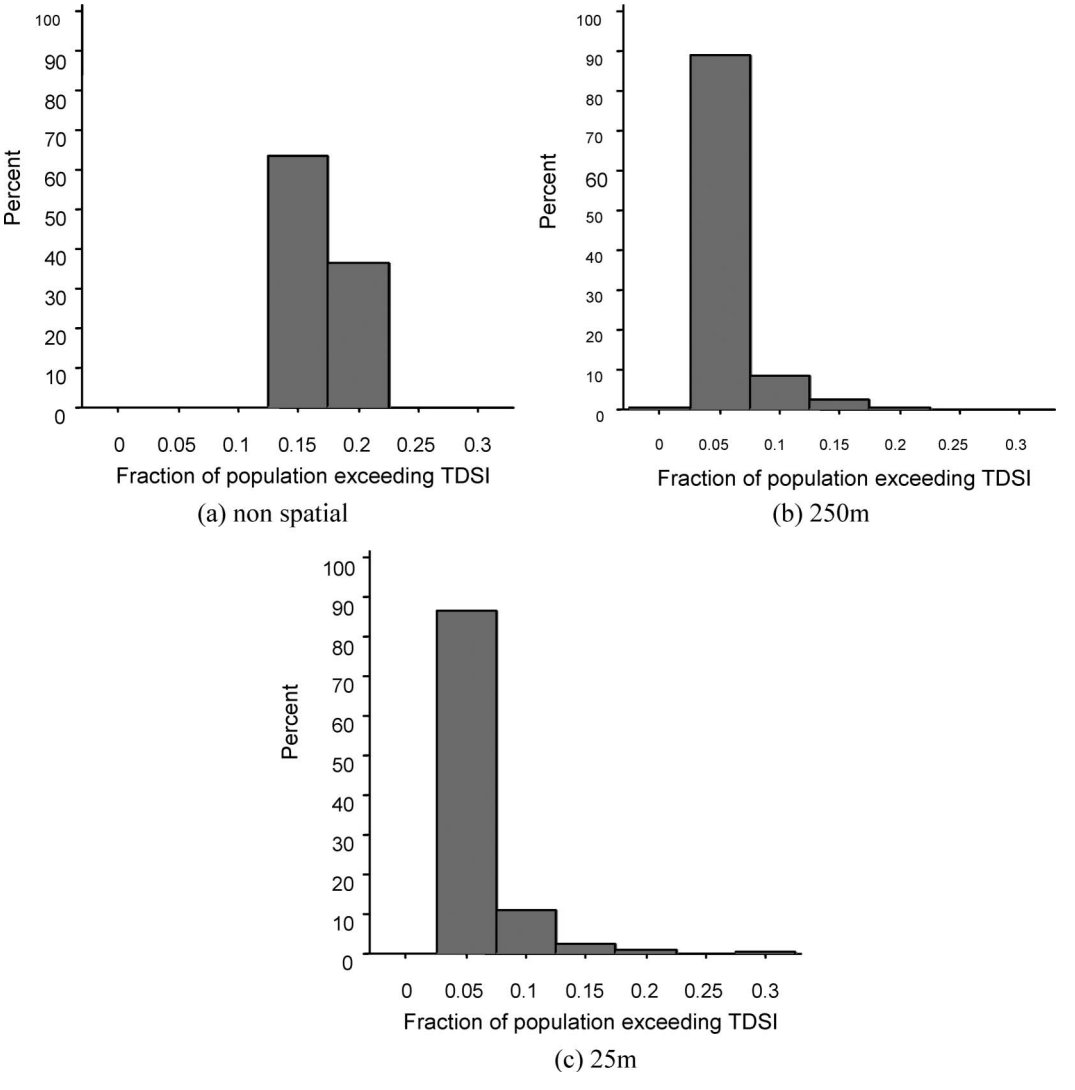

Figure 13. Proportion of the population exceeding a regulatory 'safe' cut-off for (a) nonspatial (b) 250 m and (c) 25 m support in Vasilevskaya region.

in plot (c) are quite similar up to the median and then diverge, with the nonspatial results being consistently lower than the other two. At first, the 250 m results are higher than the 25 m results, but at the very upper limits the 25 m EU results are highest.

This demonstrates that the distributions of results are, indeed, squashed as the support size increases. Nonspatial results have much higher P5s and medians and lower P95s. The 25 m EU results have the lowest P5s and highest P95s. The 250 m EU results actually have higher medians than the 25 m EUs but less than the nonspatial results. This suggests that changing support from 25 m to 250 m pushes up the lower values, which raises the medians of the soil values and in turn this raises the median exposure values.

Vegetable consumption is now included in the exposure estimates. There is a chance that due to variable pH, which will also change according to support, and hence variable CF_{veg}, the support effect may be disguised: higher pH leads to less intake from vegetables and lower pH increases intake from vegetables. However, it seems, from figure 13 that support does affect the results still. This figure shows the proportion of population which exceed the regulatory safe daily intake of Cd. The 1000 estimates on the nonspatial scale are tightly bunched, and the variation is low. The actual fraction estimated is generally higher than at the smaller supports. There appears little difference at the 250 m and 25 m supports, but the estimates are very slightly higher at the 25 m support.

These results demonstrate the differences in risk estimates that can be achieved by using different support sizes for calculating the results. An important implication of this is that the support size on which the work is undertaken should be agreed between the risk assessor and client before the assessment begins, otherwise it would be possible to manipulate the results to paint a better or worse picture as the interested party desires.

Finally, the map in figure 14 shows the spatial distribution of the population estimated to be over a regulatory 'safe' cut-off in each EU. Knowing this spatial distribution will greatly help in the efficient targeting of the clean up operation, should one be required. For most efficient reduction of numbers of the population exceeding the cut-off, one can target EUs with the highest number of overexposed individuals.

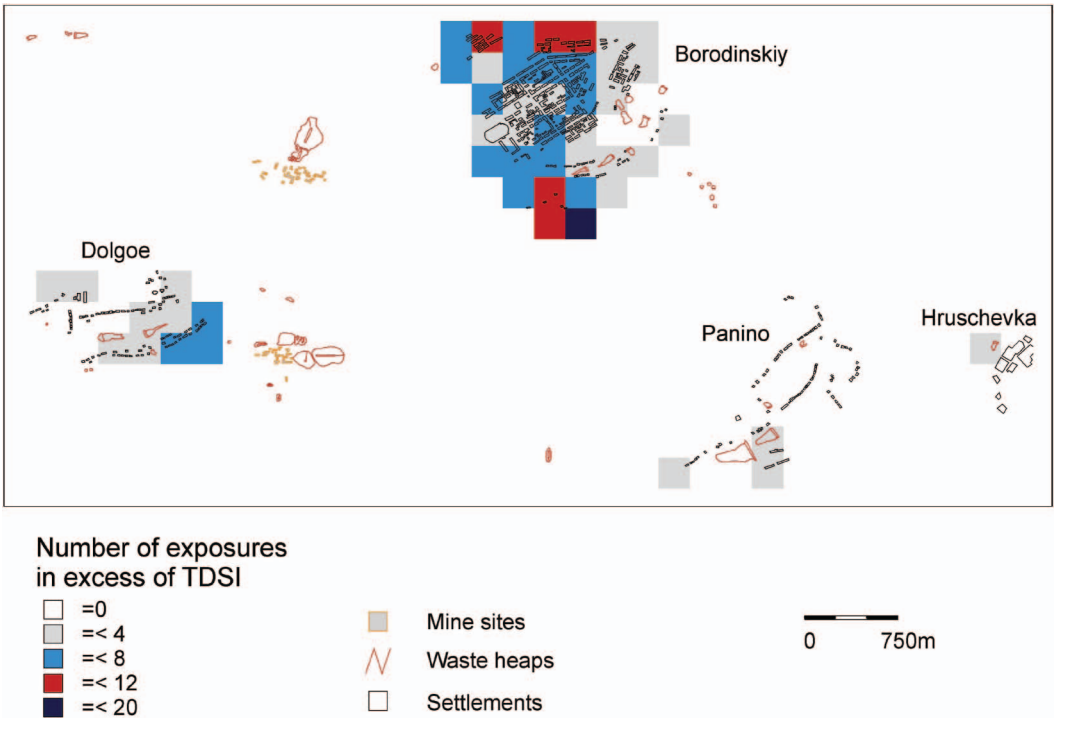

Figure 14. Spatial distribution of the median estimate for number of people per EU who exceed the regulatory 'safe' cut-off at the 250-m support size in the Vasilevskaya region.

4. Conclusions

Overall, the two case studies have demonstrated the effect of support when calculating exposure from contaminated soil in a spatially explicit manner. It has been shown that choice of support can have large effects on the number of people in the population which are classed as being over a regulatory 'safe' exposure level. It is important to choose the support in advance of the assessment to avoid tailoring results to suit an interested party. Mapping the results shows the places with the highest density of at-risk people, hence allows for targeting of any clean up measures in an efficient way.

Both Gai and Vasilevskaya case studies have demonstrated how support size and spatial distribution of people in the contaminated region can, in combination, affect the results of a risk assessment. Working at a smaller support, when estimating soil contaminant values leads to more uncertain soil concentrations. The smaller the support, the more variable the soil concentrations predicted. This is well known in geostatistics as the support effect.

For the Cd risk assessment in the Vasilevskaya region, extreme exposure estimates, estimated by the upper 95th percentile estimate for each person in the population, are more variable when calculated for a 50 m EU than when a 500 m EU is assumed, or when the average soil concentration for the region is taken. This is a direct consequence of the change in soil concentration estimates to which the population is exposed.

Median exposure estimates are less noticeably different from one support to the next. Median estimates are more stable than the extremes. When using a critical cut-off (TDSI) with the median ADE estimates it is possible, due to the support effect and the position of the critical TDSI value within the calculated ADE distribution, for results to appear worse at the median level with a larger support size than with the small support size. This is because we are not looking at the size of the excesses, just counting the number in excess of the TDSI.

Because of these subtle differences, it is important for the risk assessor and risk manager to set the criteria for judging the risks before the assessment begins to ensure that the results cannot be tailored to serve a cause.

Knowing the spatial distribution of the excess exposures allows clean up to be targeted at the highest numbers, so as to make for an efficient reduction in the number of people in the population exceeding the TDSI.

Acknowledgements

We thank the Moscow State Mining University for providing the soil data for the two case studies. This research was funded by EU grant no. ICA2-1999-10072; the authors thank the EU for their support of this research.

References

Clifford, P.A., Barchers, D.E., Ludwig, D.F., Sielken, R.L., Klingensmith, J.S., Graham, R.V. and Banton, M.I., An approach to quantifying spatial components of exposure for ecological risk assessment. *Environ. Toxicol. Chem.*, 1995, **14**, 895–906.

DEFRA & EA, Contaminants in soil: Collation of toxicological data and intake values for humans. R&D publication no. CLR9, Department for Environment, Food & Rural Affairs and the Environment Agency, Bristol, 2002.

DEFRA & EA, The contaminated land exposure assessment model (CLEA): Technical basis and algorithms. R&D publication no. CLR10, Department for Environment, Food & Rural Affairs and the Environment Agency, Bristol, 2002.

DEFRA & EA, Soil guideline values for nickel contamination. R&D publication no. SGV7, Department for Environment, Food & Rural Affairs and the Environment Agency, Bristol, 2002.

DEFRA & EA, Soil guideline values for cadmium contamination. R&D publication no. SGV3, Department for Environment, Food & Rural Affairs and the Environment Agency, Bristol, 2002.

DEFRA & EA, Contaminants in soil: Collation of toxicological data and intake values for humans: Nickel. R&D publication no. TOX8, Department for Environment, Food & Rural Affairs and the Environment Agency, Bristol, 2002.

Deutsch, C.V. and Journel, A.G., *GSLIB Geostatistical Software Library and User's Guidel*, 1998 (Oxford University Press: New York).

Flatman, G.T., Brown, K.W. and Mullins, J.W., Probabilistic spatial contouring of the plume around a lead smelter, in *Proceedings of the Sixth National Conference on Management of Uncontrolled Hazardous Waste Sites*, pp. 442 – 448, 1985 (Hazardous Materials Control Research Institute: Washington, DC).

Gay J.R. and Korre A., A spatially-evaluated methodology for assessing risk to a population from contaminated land. *Environ. Pollut*., 2006, **142**, 227 – 234.

Geovariances, Isatis, Version 6.0.4., 2007 (Geovariances: Avon Cedex, France).

Hope, B.K. A case study comparing static and spatially explicit ecological exposure analysis methods. *Risk Analysis*, 2001, **21**, 1001 – 1010.

Hygienic Standards, Tentative allowable concentrations (TAC) of heavy metals and arsenic in soils. Appendix N1 to the list of PDK and TAC. Government report N6229-91 Hygienic Standards, Moscow, 2001.

Kooistra, L., Leuven, R., Nienhuis, P.H., Wehrens, R. and Buydens, L.M.C., A procedure for incorporating spatial variability in ecological risk assessment of Dutch River floodplains. *Environ. Manage*., 2001, **28**, 359 – 373.

Korre, A., Durucan, S. and Koutroumani, A., Quantitative-spatial assessment of the risks associated with high Pb loads in soils around Lavrio, Greece. *Appl. Geochem*., 2002, **17**, 1029 – 1045.

Leonte, D. and Schofield, N., Evaluation of a soil contaminated site and clean-up criteria: A geostatistical approach. In *Geostatistics for Environmental and Geotechnical Applications, ASTM STP 1283*, edited by R.M. Srivastava, S. Rouhani, M.V. Cromer, A.J. Desbarats and A.I. Johnson, pp. 133 – 145, 1996 (American Society for Testing and Materials).

Linkov, I., Grebenkov, A. and Baitchorov, V.M. Spatially explicit exposure models: Application to military sites. *Toxicol Indust Health*, 2001, **17**, 230 – 235.

McKenna, S.A., Geostatistical approach for managing uncertainty in environmental remediation of contaminated soils: Case study. *Environ. Eng. Geosci*., 1998, **4**, 175 – 184.

Meshalkina, J.L., Stein, A. and Makarov, O.A., Spatial variability of soil contamination around a sulphureous acid producing factory in Russia. *Water Air Soil Pollut*., 1996, **92**, 289 – 313.

Moir A.M. and Thornton I., Lead and cadmium in urban allotment and garden soils and vegetables in the United-Kingdom. *Environ. Geochem. Health*, 1989, **11**, 113 – 119.

Tristan, E., Demetriades, A., Ramsey, M.H., Rosenbaum, M.S., Stavrakis, P., Thornton, I., Vassiliades, E. and Vergou, K., Spatially resolved hazard and exposure assessments: An example of lead in soil at Lavrion, Greece. *Environ. Res*., 2000, **82**, 33 – 45.

USEPA, Risk assessment guidance for superfund (RAGS), Vol. I, Human Health Evaluation Manual, Part A. United States Environmental Protection Agency, 1989.